Skeletal Radiol (2017) 46:665–673
DOI 10.1007/s00256-017-2598-5

SCIENTIFIC ARTICLE

Fatty rind of intramuscular soft-tissue tumors of the extremity: is it different from the split fat sign?

Jinkyeong Sung[1] · **Jee-Young Kim**[1]

Received: 14 November 2016 / Revised: 31 December 2016 / Accepted: 8 February 2017 / Published online: 2 March 2017

Abstract
Objective To analyze intramuscular soft-tissue tumors with fatty rind, and to evaluate the difference between fatty rind and split fat sign on magnetic resonance imaging (MRI).
Materials and methods We retrospectively analyzed 50 pathologically confirmed intramuscular masses on MRI. We evaluated the distribution and shape of fatty rind and muscle atrophy.
Results Fatty rind was found more frequently in benign lesions (80% [36 out of 45]) compared with malignant lesions (25% [1 out of 5]; $P = 0.013$). Thirty-six benign lesions were peripheral nerve sheath tumors (PNSTs; $n = 19$), hemangiomas ($n = 11$), myxomas ($n = 2$), ganglion cysts ($n = 2$), giant cell tumor ($n = 1$), and leiomyoma ($n = 1$). One malignant lesion was a low-grade fibromyxoid sarcoma. In all masses with fatty rind, fat was confined to the proximal and the distal ends. In 12 cases, complete or partial circumferential fatty rind was also noted. Fatty rinds at both ends showed crescent, triangular, or combined shape. The prevalence of crescent-shaped fatty rind was significantly higher in benign PNST (17 out of 38) compared with the other tumors (1 out of 32; $P < 0.001$). Complete circumferential fat was noted only in hemangioma ($n = 5$). Triangular fatty rind was related to peripheral location of the mass or muscle atrophy.
Conclusion Most intramuscular tumors with fatty rinds were benign, and PNST was the most common tumor type. Fatty rind could be caused by displaced neurovascular bundle fat, fatty atrophy of the muscle involved, or intermuscular or perimysial fat. Crescent-shaped fatty rind was noted more frequently in benign PNSTs.

Keywords Intramuscular soft tissue tumor · Fatty rind · Magnetic resonance imaging · Peripheral nerve sheath tumors

Introduction

Split fat sign represents fine fat deposition around the lesion and is usually seen as a tapered rim of fat signal adjacent to the proximal and distal ends of the lesion on T1-weighted coronal or axial images. Split fat is produced as a mass grows and normal intermuscular fat is displaced and effaced around the lesion. Split fat sign is known to be a typical magnetic resonance imaging (MRI) feature of peripheral nerve sheath tumors (PNSTs) [1–5]. This sign is not specific to PNSTs, but is commonly seen in benign soft-tissue tumors that originate from the intermuscular space.

In intramuscular tumors, only a few studies have investigated split fat sign in intramuscular PNSTs and fatty atrophy around an intramuscular myxoma [6–11]. However, whether the appearance of fat around the intramuscular PNSTs is the same as that of intermuscular PNSTs is uncertain, and the cause of fat around the intramuscular PNSTs remains unclear. In addition, whether other intramuscular tumors show fat around the mass has not been evaluated. Thus, the purpose of our study was to analyze intramuscular soft-tissue tumors with fatty rind, and to evaluate the difference between fatty rind and split fat sign on MRI.

Materials and methods

This retrospective study was approved by our institutional review board. The requirement for informed consent was waived because of the retrospective nature of this study.

✉ Jee-Young Kim
jeeykim@catholic.ac.kr

[1] Departments of Radiology, St. Vincent's Hospital, College of Medicine, The Catholic University of Korea, 93, Jungbu-daero, Paldal-gu, Suwon, Gyeonggi-do 16247, South Korea

Table 1 Clinical and MRI findings of intramuscular tumors

Patient number	Age/sex	Pathology	Duration	Muscle involved	Maximum diameter (cm)	Fatty rind (proximal)	Fatty rind (distal)	Fatty rind (circumferential)
1	71/female	Schwannoma	1 month	Flexor hallucis longus	3	C + T (A)	C	–
2	28/male	Schwannoma	1 year	Pronator teres	1.5	T (A)	T (P)	–
3	62/female	Schwannoma	1.5 months	Rectus femoris	2	C	C	–
4	64/female	Schwannoma	2 years	Rectus femoris	4	C	T (A)	–
5	33/male	Schwannoma	1 month	Vastus intermedius	2.6	C + T (p)	C + T (p)	–
6	14/male	Schwannoma	3 years	Abductor pollicis longus	1.7	C + T (P)	T (P)	–
7	37/female	Ancient schwannoma	10 years	Biceps femoris, short head	5.3	T (A)	T (P, A)	Partial
8	52/male	Schwannoma	2 years	Vastus medialis	1.4	C	C + T (p)	–
9	38/male	Schwannoma	2.5 years	Soleus	3.2	C + T (P)	C	–
10	37/female	Schwannoma	4 months	Vastus lateralis	3.6	T (A)	C	Partial
11	73/male	Ancient schwannoma	2 years	Sartorius	3.5	T (A)	T (P, A)	–
12	44/female	Schwannoma	1 month	Soleus	3.7	C	C	–
13	37/male	Schwannoma	1 year	Deltoid	1.6	T (P, A)	T (P, A)	–
14	69/female	Schwannoma	2 years	Deltoid	3	T (P, A)	T (P, A)	Partial
15	61/female	Schwannoma	3 years	Abductor digiti minimi	5	C	T (P)	–
16	50/male	Neurofibroma	5 years	Gracilis	6.6	C	C + T (P, A)	–
17	54/female	Neurofibroma	Incidental	Adductor magnus	8.8	C	C	–
18	41/male	Neurofibroma	3 months	Rectus femoris	5.5	C	C	–
19	27/female	Neurofibroma	1 month	Gracilis	2.9	C	C	–
20	44/female	Hemangioma	5 years	Soleus	2.4	T (P, A)	T (P, A)	Complete
21	8/male	Hemangioma	3 months	Abductor digiti minimi	2.5	–	T (A)	–
22	21/male	Hemangioma	4 years	Lumbricals	1.5	T (P, A)	C	Partial
23	30/male	Hemangioma	3 years	Soleus	3.4	T (A)	T (P, A)	–
24	22/male	Hemangioma	15 years	Vastus lateralis	5.7	T (P)	T (P)	Complete
25	27/male	Hemangioma	3 years	Gluteus maximus	7.6	T (A)	T (P, A)	Complete
26	30/male	Hemangioma	3 years	Soleus	4.1	T (A)	T (P, A)	–
27	33/male	Hemangioma	3 weeks	Peroneus	4.8	C + T (P)	T (P)	–
28	35/female	Hemangioma	1 month	Soleus	1.9	T (A)	T (A)	Complete
29	23/female	Hemangioma	20 years	Triceps brachii, medial head	2.8	T (A)	T (P)	Complete
30	38/female	Hemangioma	3 years	Soleus	2.7	T (A)	T (A)	–
31	40/female	Leiomyoma	2 months	Soleus	1.8	T (P, A)	T (P, A)	Partial
32	39/female	Myxoma	Incidental	Longissimus dorsi	2.5	T (P)	T (A)	–
33	48/male	Myxoma	3 years	Vastus medialis	5.3	T (P, A)	T (A)	–
34	51/female	Ganglion cyst	8 months	Soleus	2.8	–	T (P)	–
35	38/male	Ganglion cyst	2 years	Soleus	3.2	–	C + T (A)	–
36	14/female	Giant cell tumor	6 months	Triceps brachii, lateral head	3.4	T (P, A)	T (P)	Partial
37	63/female	Low-grade fibromyxoid sarcoma	1 year	Gluteus maxims	11	C + T (P)	C + T (A)	Partial

C crescent-shaped, *T* triangular, *P* peripheral location of the muscle belly, *p* perimysial location, periphery of the muscle bundle

A: Atrophy

Patient selection

We searched and reviewed clinical and MRI databases at our medical center between January 2006 and February 2016. We identified all patients who had a pathologically confirmed intramuscular mass confined to one muscle. Twenty-three patients with lipoma, atypical lipomatous tumor, or liposarcoma were excluded owing to difficult delineation of the fatty rind and mass. Fifty consecutive patients who had a pathologically confirmed intramuscular mass on MRI were identified. The study group consisted of 24 men and 26 women (mean age, 40.9 years; age range, 6–73 years). Clinical presentation, duration, history of trauma or surgery, and laboratory data were reviewed.

Fig. 1 A 22-year old man with a hemangioma in the vastus lateralis muscle (patient 24). **a**, **b** Coronal T1-weighted images show triangular fatty rinds (*arrows*) at the proximal and distal ends of the mass, related to the peripheral location of the tumor. A complete circumferential fatty rind (*arrowheads*) surrounds the mass

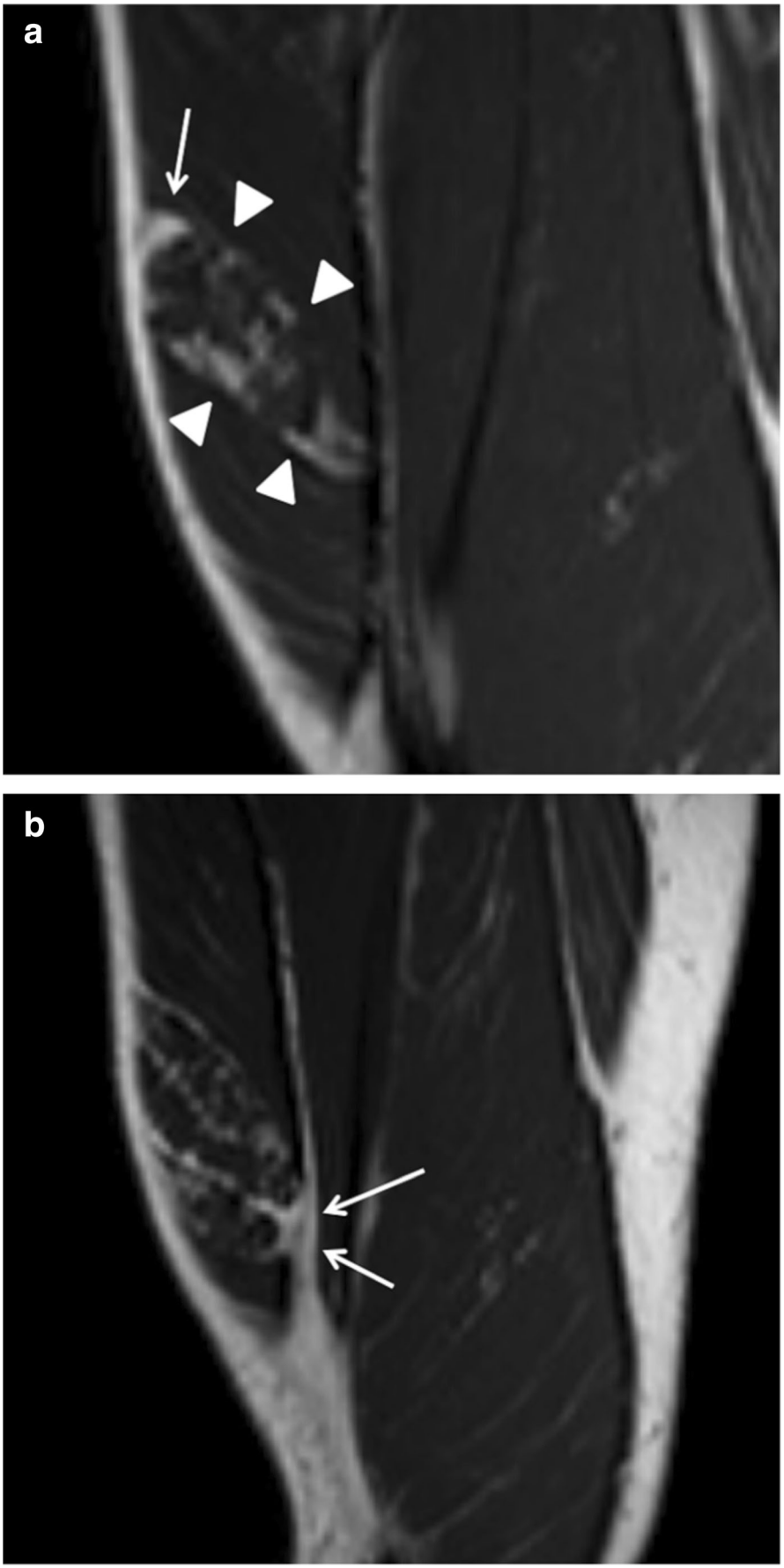
a
b

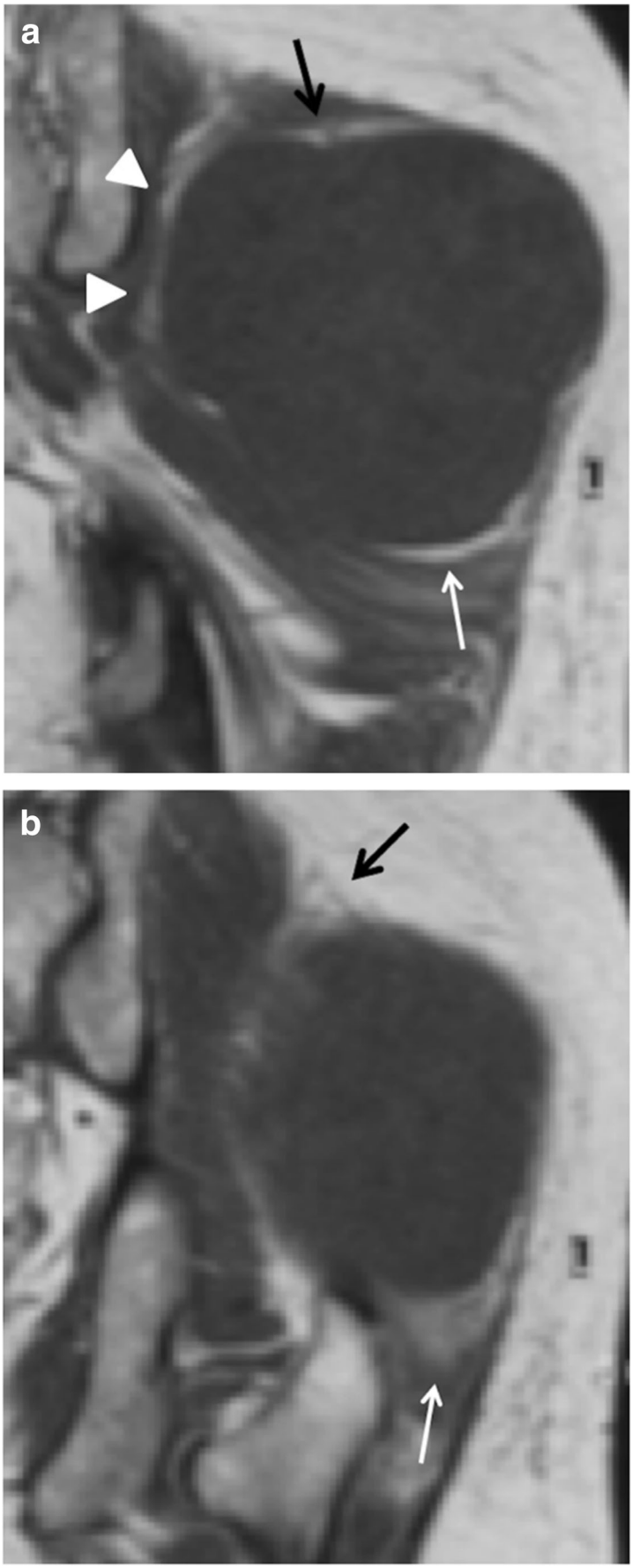
a
b

◀ **Fig. 2** A 63-year old woman with a low-grade fibromyxoid sarcoma in the gluteus maximus muscle (patient 37). **a** Coronal T1-weighted image in the central portion of the mass reveals crescent-shaped fatty rind (*arrows*) at both the proximal and distal ends of the mass. Partial circumferential fat (*arrowheads*) is seen along the central portion of the tumor. **b** Coronal T1-weighted image in the paracentral portion shows triangular fatty rind (*black arrow*) at the proximal end of the mass, which is related to the peripheral location of the tumor. Another triangular fatty rind (*white arrow*) is noted in the distal portion of the mass, which is related to the muscle atrophy

Imaging technique

In all cases, MRI was performed with 1.5-T (Gyroscan Intera, Philips Medical Systems, Best, The Netherlands, or Signa, GE Medical Systems, Milwaukee, WI, USA) and 3.0-T (Magnetom Verio, Siemens, Erlangen, Germany) scanners. MRI protocols included spin-echo T1-weighted (TR/TE range, 325–700/10–21 at 1.5 T, 479–664/10–11 at 3.0 T), spin-echo T2-weighted with and without fat suppression (TR range/TE range, 2,000–4,200/70–100 at 1.5 T, 2,300–5,340/63–78 at 3.0 T), and gadolinium enhancement of T1-weighted images. Axial, coronal, and sagittal images were obtained for all patients. Gadolinium-enhanced T1-weighted images were obtained in at least two orthogonal planes. The fat-suppression technique was used for gadolinium-enhanced T1-weighted images.

Imaging analysis

Two musculoskeletal radiologists with 20 and 5 years of experience in musculoskeletal radiology respectively reviewed the MRI features of each lesion by consensus. The muscle involved and the size of all masses was assessed. Fatty rind was defined as a fat signal around the mass.

We analyzed the distribution and shape of fatty rind around the mass and the location of the mass in the muscle belly. We classified the distribution of fatty rind according to the covered surface: localized type (<50%) and circumferential type (partial: 50% to <100%, complete: 100%). The shape of fatty rind was classified into three types: crescent, triangular, or combined crescent and triangular. Crescent shape was defined as a thin curvilinear fat deposition. Triangular shape indicated a localized, condensed fat deposition, not curvilinearly. When both crescent and triangular fatty rind coexisted, it was regarded as a combined type. In addition, we assessed the location of the mass in the muscle belly. When the tumor abutted the fascia, it was classified to the peripheral location of the muscle belly. If the tumor abutted the perimysium within the muscle belly, it was classified to the perimysial location (periphery of the muscle bundle). We also analyzed the fatty atrophy of the muscle involved, which was defined as the decreased muscle volume and fat deposition next to the mass.

Pathological analysis

After imaging, all 50 patients underwent complete excision of the masses. An experienced pathologist examined the excised specimens, and a final diagnosis was established based on histological morphology and immunohistochemistry.

Statistical analysis

The prevalence of fatty rind in intramuscular benign and malignant lesions was compared using Fisher's exact test. The Chi-squared test or Fisher's exact test was used for the comparison of fatty rind types from different lesions. The Mann–Whitney *U* test was used to compare the duration of the mass between tumors with fatty atrophy and tumors without fatty atrophy. For all tests, $P < 0.05$ was considered indicative of a statistically significant difference.

Results

Forty-five cases were benign and five cases were malignant. Among them, 13 cases (mean age, 47 years; age range, 6–72 years) did not have a fatty rind (26% [13 out of 50]). Nine benign lesions were hemangioma ($n = 2$), ganglion cysts ($n = 2$), heterotopic ossification ($n = 2$), hematoma ($n = 1$), myxoma ($n = 1$), and angioleiomyoma ($n = 1$). Four malignant lesions were rhabdomyosarcoma ($n = 1$), alveolar soft part sarcoma ($n = 1$), metastatic adenocarcinoma ($n = 1$), and high-grade myxofibrosarcoma ($n = 1$). Thirty-seven cases (mean age, 40.4 years; age range, 8–73 years) had fatty rind (74% [37 out of 50]). Thirty-six benign lesions were benign PNSTs; ($n = 19$, 15 schwannoma and 4 neurofibroma), hemangiomas ($n = 11$), myxomas ($n = 2$), ganglion cysts ($n = 2$), giant cell tumor (GCT; $n = 1$), and leiomyoma ($n = 1$). One malignant lesion was a low-grade fibromyxoid sarcoma. Among intramuscular lesions (confined to one muscle), the fatty rind was found more frequently in benign lesions (80% [36 out of 45]) compared with malignant lesions (25% [1 out of 5]; $P = 0.013$).

Clinical and MRI findings of intramuscular tumors with fatty rind are summarized in Table 1. All except 2 of the patients presented with a chief complaint of a palpable mass lasting more than 3 weeks and up to 20 years. Four patients with hemangioma complained of a painful mass. In 1 patient with a neurofibroma (case 17) and 1 patient with myxoma (case 32), the mass was found incidentally during evaluation of breast cancer and herpes zoster respectively. Among cases of neurogenic tumors, only 5 patients demonstrated a positive Tinel's sign. One patient presented with neurofibroma and had neurofibromatosis type 1. None of the patients had antecedent traumas or previous surgery, and all laboratory results were unremarkable.

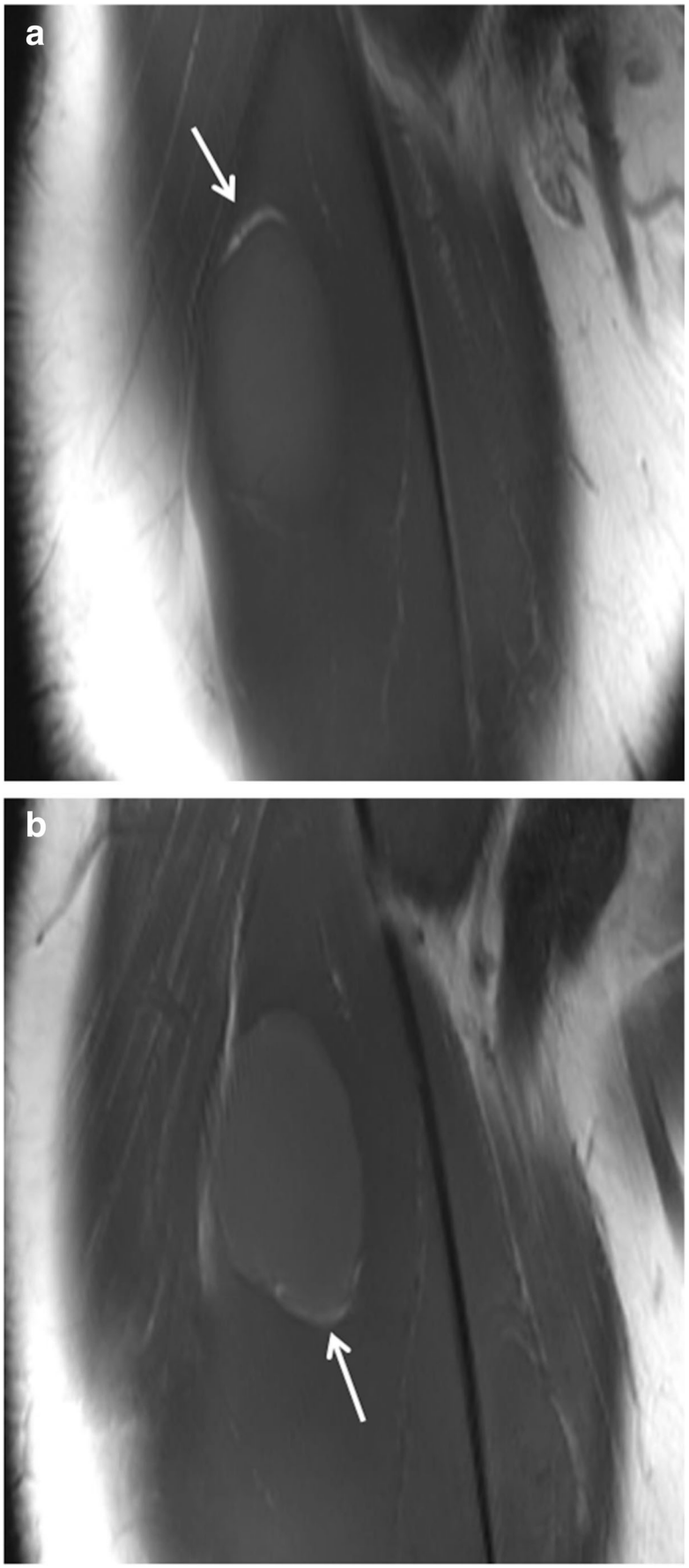
a
b

◀ **Fig. 3** A 41-year-old man with a neurofibroma of the rectus femoris muscle (patient 18). **a**, **b** Coronal T1-weighted images reveal crescent-shaped fatty rind (*arrow*) at both the proximal and distal ends of the mass

The mean maximum diameter of benign tumors with a fatty rind was 3.5 cm (1.4–8.8 cm), and the maximum diameter of malignant tumors with a fatty rind was 11 cm. On MRI, all tumors with a fatty rind showed fat that was confined to the proximal and distal ends of the lesions. Twenty-five cases showed localized type fatty rinds, and 12 cases showed circumferential type fatty rinds. Circumferential fatty rind was found in hemangioma ($n = 6$), PNST ($n = 3$), leiomyoma ($n = 1$), GCT ($n = 1$), and low-grade fibromyxoid sarcoma ($n = 1$; Figs. 1, 2). The prevalence of circumferential fatty rind was higher in hemangioma (6 out of 11) than in the other tumors (6 out of 26; $P = 0.122$), but this result was not statistically significant. Complete circumferential fat was noted only in hemangioma ($n = 5$).

For shape analysis, each end was counted separately. Among 37 tumors with 74 ends, a total of 71 ends had fatty rinds. Crescent-shaped fatty rind ($n = 18$) was present in PNSTs ($n = 17$) and hemangioma ($n = 1$; Fig. 3). The prevalence of crescent-shaped fatty rind was significantly higher in benign PNSTs (17 out of 38) compared with the other tumors (1 out of 32; $P < 0.001$). Triangular fatty rinds ($n = 53$) were present in all tumor types. Peripheral location of muscle belly ($n = 19$), fatty atrophy ($n = 14$), peripheral location of both muscle belly and fatty atrophy ($n = 17$), and perimysial location (peripheral location of the muscle bundle; $n = 3$) contributed to the triangular fatty rind formation (Figs. 1, 2, and 4). Among them, the combined crescent and triangular shape ($n = 10$) was noted in PNSTs ($n = 7$), hemangioma ($n = 1$), ganglion cyst ($n = 1$), and low-grade fibromyxoid sarcoma ($n = 1$; Fig. 2). The duration of the mass with fatty atrophy was longer than that without fatty atrophy, but this result was not statistically significant ($P = 0.196$).

Discussion

In our study, fatty rind was more frequently observed in benign intramuscular tumors than in malignant intramuscular tumors. In all tumors with fatty rind, the fat was confined to the proximal and distal ends, with or without circumferential fat. Fatty rinds at both ends showed crescent, triangular or combined crescent and triangular shapes. Crescent-shaped fatty rind was noted more frequently in benign PNSTs, and circumferential fatty rind was most commonly seen in hemangiomas. Triangular-shaped fatty rind was related to the peripheral location of the mass or atrophy of the muscle involved.

Normally, fat is interposed between muscles, around the neurovascular bundle. When a tumor that originates in the intermuscular space grows slowly, it is surrounded by fat, particularly with a tapered rim of fat adjacent to the proximal and distal ends of the lesion [2]. In intramuscular tumors, a few studies have described split fat signs in intramuscular schwannomas [6–8]. However, because radiology images do not show gross fat in the intramuscular region, we thought that split fat sign may be not an appropriate term for intramuscular lesions. Therefore, we designated the fat around the intramuscular mass as a fatty rind.

Zhang et al. reported that no intramuscular malignant soft-tissue tumors showed the split fat sign in their study [8]. In our study, the prevalence of fatty rind was significantly higher in benign tumors than in malignant tumors. However, in our cases, there was one malignant tumor with a fatty rind. We suspected that the low malignancy grade of the tumor (low-grade fibromyxoid sarcoma) that showed slow growth (1 year) might have induced the fatty rind.

There were three different fatty rind shapes at the ends of masses in this study: crescent, triangular, and combined crescent and triangular. The crescent-shaped fatty rind was sharply defined along the proximal and distal margins of the tumors and was commonly visualized in PNSTs. Kransdorf and Murphey suggested that the neurovascular bundle is normally surrounded by fat, and a slow-growing mass that arises from the neurovascular bundle tends to maintain a rim of fat [2, 12]. We propose that this theory supports the formation of the crescent-shaped fatty rind. This type of fatty rind was not associated with atrophy of the muscle involved on MRI. The crescent-shaped fatty rind in intramuscular PNSTs has not been previously described. In addition to benign PNSTs, crescent-shaped fatty rind was also seen in hemangioma and ganglion cysts. Ganglion cysts can occasionally grow along the neurovascular bundle. The crescent-shaped fatty rind could be used to differentiate soft-tissue tumors that originate from neurovascular bundles, especially PNSTs, from other intramuscular soft-tissue tumors. We assumed that the crescent type of malignant tumor was the fat from the atrophy of the muscle involved and the fat of the intermuscular fascia. The fast expansion (compared with the benign tumor) of the tumor volume in the malignant tumor can reduce the fat deposit and make it appear to be a thin, curvilinear shape.

In our study, the triangular fatty rind was visualized with two mechanisms. First, the fat of the intermuscular space or perimysium encircling muscle bundles appeared to be a triangle. As tumors grew to the periphery of the muscle belly or muscle bundle, the normal fat of the intermuscular space or perimysium was displaced, creating the triangular fatty rind. Second, the triangular shape was the fat from the atrophy of the muscle involved. Because the duration of the mass with fatty atrophy was longer that that without fatty atrophy, although this result was not statistically significant ($P = 0.196$), it is possible that the mass effect of slow-growing tumor and delayed detection related to deep intramuscular location may have contributed to muscle atrophy. Denervation changes in

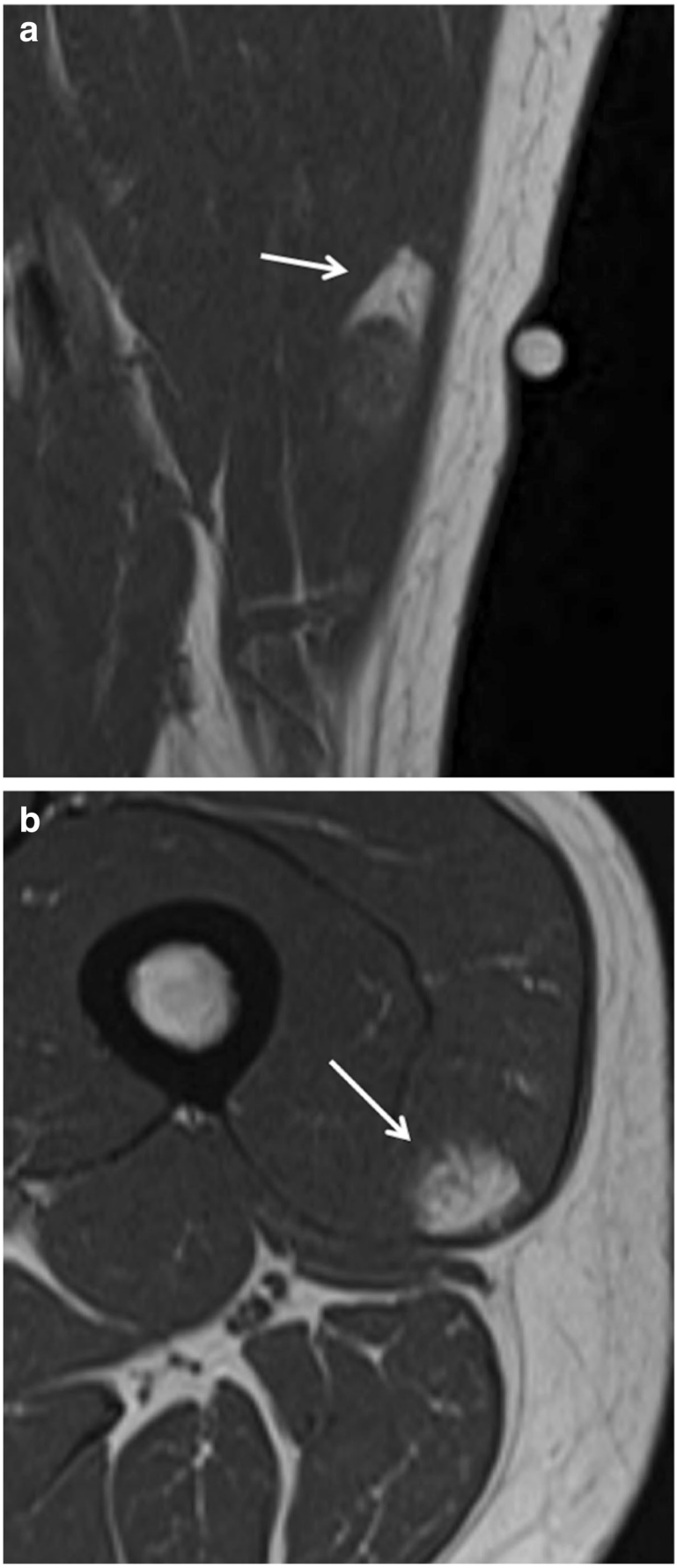
a
b

◀ **Fig. 4** A 37-year-old woman with a schwannoma in the vastus lateralis muscle (patient 10). **a** Coronal T1-weighted image shows a triangular-shaped fatty rind (*arrow*) at the proximal end of the mass. **b** Corresponding axial T1-weighted image demonstrates fatty atrophic change (*arrow*) in the muscle proximal to the mass

the nerves that involve the tumor (such as PNST) could also have caused the muscle atrophy. In a few previous studies of intramuscular myxoma, fat tissue surrounding the mass histologically corresponded to atrophic change of muscle due to the infiltrative pattern and slow tumor growth [10, 11]. However, these studies have not described the shape and distribution of the fat rinds.

When the possible mechanisms mentioned above are present together, the shape of the combined type can be visualized on the image. In all tumors with fatty rind, the fat around the mass was deposited adjacent to one or both ends of the masses. In the crescent type, we hypothesized that fat along the neurovascular bundle might have been displaced to the more spacious end of the mass. In the triangular type, we hypothesized that muscle atrophy might have progressed along the direction of tumor growth or that muscle atrophy might have been masked by the mass effect of the tumor in the central portion.

In some cases, the fatty rind encircled the mass, which formed a circumferential shape. This was most commonly seen in hemangioma, and the complete circumferential shape was seen only in hemangioma. Partial circumferential shape was also noted in schwannoma, leiomyoma, giant cell tumor of the tendon sheath, and low-grade fibromyxoid sarcoma. We thought that the circumferential shape could be attributable to the multi-directional mass effect of the vessel or tumor infiltration, not just along the long axis of the tumor, as in PNSTs. In hemangioma, reactive fat overgrowth and muscle atrophy related to chronic vascular insufficiency may be prominent and completely encircle the mass [13].

There were some limitations to our study. Pathological confirmation of peripheral fatty tissue was not performed because of the retrospective nature of our study. However, we propose that MRI is sufficient to show and analyze fat around intramuscular soft-tissue tumors. Despite these limitations, we believe that our results contribute to a better understanding of fatty rind in intramuscular soft-tissue tumors and approaches for differentiation.

In conclusion, most of the intramuscular tumors with fatty rinds were benign, and the most common tumor was PNST. The crescent-shaped fatty rind may have been caused by the displaced fat of a neurovascular bundle. Triangular fatty rind was caused by fatty atrophy of the muscle involved or intermuscular or perimysial fat. The crescent-shaped fatty rind was noted more frequently in benign PNSTs than in other intramuscular tumors. The circumferential fatty rind was most commonly seen in hemangiomas.

Compliance with ethical standards

Conflicts of interest The authors have no conflicts of interest to declare.

Funding No funding was necessary to carry out this study.

Ethical approval All procedures performed in studies involving human participants were carried out in accordance with the ethical standards of the institutional and/or national research committee and with the 1964 Declaration of Helsinki and its later amendments or comparable ethical standards.

References

1. Stull MA, Moser Jr RP, Kransdorf MJ, Bogumill GP, Nelson MC. Magnetic resonance appearance of peripheral nerve sheath tumors. Skeletal Radiol. 1991;20:9–14.
2. Abreu E, Aubert S, Wavreille G, Gheno R, Canella C, Cotten A. Peripheral tumor and tumor-like neurogenic lesions. Eur J Radiol. 2013;82:38–50.
3. Murphey MD, Smith WS, Smith SE, Kransdorf MJ, Temple HT. From the archives of the AFIP. Imaging of musculoskeletal neurogenic tumors: radiologic-pathologic correlation. Radiographics. 1999;19:1253–80.
4. Pilavaki M, Chourmouzi D, Kiziridou A, Skordalaki A, Zarampoukas T, Drevelengas A. Imaging of peripheral nerve sheath tumors with pathologic correlation: pictorial review. Eur J Radiol. 2004;52:229–39.
5. Chee DW, Peh WC, Shek TW. Pictorial essay: imaging of peripheral nerve sheath tumours. Can Assoc Radiol J. 2011;62:176–82.
6. Salunke AA, Chen Y, Tan JH, et al. Intramuscular schwannoma: clinical and magnetic resonance imaging features. Singapore Med J. 2015;56:555.
7. Shimose S, Sugita T, Kubo T, et al. Major-nerve schwannomas versus intramuscular schwannomas. Acta Radiol. 2007;48:672–7.
8. Zhang Z, Deng L, Ding L, Meng Q. MR imaging differentiation of malignant soft tissue tumors from peripheral schwannomas with large size and heterogeneous signal intensity. Eur J Radiol. 2015;84:940–6.
9. Bancroft LW, Kransdorf MJ, Menke DM, O'Connor MI, Foster WC. Intramuscular myxoma: characteristic MR imaging features. Am J Roentgenol. 2002;178:1255–9.
10. Luna A, Martinez S, Bossen E. Magnetic resonance imaging of intramuscular myxoma with histological comparison and a review of the literature. Skeletal Radiol. 2005;34:19–28.
11. Murphey MD, McRae GA, Fanburg-Smith JC, Temple HT, Levine AM, Aboulafia AJ. Imaging of soft-tissue myxoma with emphasis on CT and MR and comparison of radiologic and pathologic findings. Radiology. 2002;225:215–24.
12. Kransdorf MJ, Murphey MD. Imaging of soft tissue tumors. 2nd ed. Philadelphia: Lippincott Williams & Wilkins; 2006.
13. Olsen KI, Stacy GS, Montag A. Soft-tissue cavernous hemangioma. Radiographics. 2004;24:849–54.